Development and Evaluation of Ion Energy Analyzer for Energetic Ion Measurement in a Linear Plasma Device NUMBER*)

Ryosuke OCHIAI, Atsushi OKAMOTO, Takaaki FUJITA, Hideki ARIMOTO, Hiroki HACHIKUBO, Minami SUGIMOTO and Kento IIZUKA

Graduate School of Engineering, Nagoya University, Furo-cho, Chikusa-ku, Nagoya 464-8603, Japan

(Received 6 January 2020 / Accepted 26 March 2020)

In order to directly measure high energy ions in a plasma and to establish a new energetic-ion-production method, we have developed an ion energy analyzer for measuring the ion energy distribution. The analyzer is a retarding potential analyzer consisting of three grids and a collector. By applying a voltage to each grid, the electrons are retarded and the ions are separated by energy. In the measurement of the plasma with the electron density of higher than 10^{17} m^{-3}, it was found that the collector current was smaller than that deduced from the geometrical transparency of the grids. Measurement of the current flowing into each grid and a particle-in-cell simulation revealed that collector current decreased due to space charge between the 2nd and 3rd grids.

Keywords: energetic ion, high density magnetized plasma, linear plasma device, retarding potential analyzer, space charge effect

DOI: 10.1585/pfr.15.2401040

1. Introduction

Alpha particles generated by DT reaction in a magnetic confinement fusion reactor are expected to heat plasma by transferring their energy. Confining the alpha particles is necessary to keep the high temperature plasma. Therefore, study on the alpha particle transport is very important in magnetically confined nuclear fusion development.

In order to simulate the alpha particles with high energy ions, a new energetic-ion-production method is required especially for smaller devices. In these experiments, it is necessary to match the ratio of the plasma minor radius and the energetic ion Larmor radius. For example, the plasma minor radius and toroidal magnetic field strength of a typical fusion reactor are 2 m and 5 T, respectively. The ratio of the Larmor radius of alpha particles to the plasma minor radius is about 5×10^{-2}. Therefore, in a typical small device such as HYBTOK-II (toroidal magnetic field strength 0.5 T, plasma minor radius 0.1 m, density 5×10^{18} m^{-3}) [1], high energy ions of several hundred eV are required. In addition, it is necessary to emit a current density of about 1 - 10 A/m^2 in order to match the ratio between the bulk plasma density and the amount of high-energy ions generated. We are developing a new energetic-ion-production method using the linear plasma experiment device NUMBER [2], which has advantages in controllability and easiness of measurement.

In the method under development, hydrogen released from an electrode is ionized in plasma, and the ions are accelerated by sheath around the electrode. Therefore, a high density plasma of about 10^{18} m^{-3} is required to ionize and accelerate hydrogen sufficiently. In Ref. [3], the same method was adopted. Increase in H_α emission was observed when the electrode was positively biased. However, direct detection of accelerated ion was not performed. Direct measurement of generated energetic ions is important for evaluation of the method.

So, an analyzer that can separate and measure energetic ions and background plasma ions in a high-density magnetized plasma is required. As such analyzers, a retarding potential analyzer (RPA) [4] and an ion sensitive probe (ISP) [5] can be considered. In ISP the ion energy distribution is obtained by separating the particles in the plasma by their Larmor radii. However, it is difficult to measure the time variation of the ion energy distribution under the time varying external magnetic field as in typical NUMBER experiment. Because RPA obtains energy distribution by separating ions according to the electrostatic potential, the aforementioned problem does not occur. Therefore, we use RPA in this study to evaluate the generation method.

Since the energetic ion generation method requires a high density plasma ($\sim 10^{18}$ m^{-3}), two points are cared in the design of the RPA used for this measurement. The first one is the Debye shielding. Internal structure and geometry are designed considering this point. The second one is perturbation or shadow effect. Those are reflected to the outer dimension and surface of RPA. Moreover, sensitivity of the RPA should be considered in terms of high-density bulk-plasma rejection and small flux of energetic ion detection. In this paper, development of an RPA, which is suitable

author's e-mail: okamoto.atsushi@nagoya-u.jp

*) This article is based on the presentation at the 28th International Toki Conference on Plasma and Fusion Research (ITC28).

for detecting energetic ion flux in high-density plasma, is described.

Until now, RPAs applicable to high density ($\geq 10^{18}$ m^{-3}) plasma are embedded in the wall or have an outer diameter of 20 mm or more [4, 6, 7]. We have developed a compact (< 10 mm) RPA that can be measured in a high-density small diameter (< 100 mm) plasma. Experimental device is shown in Sec. 2. Details of RPA are described in Sec. 3 followed by results and discussion in Sec. 4, and summarized in Sec. 5.

2. Experimental Device

Experiments were performed using a linear plasma device NUMBER as schematically shown in Fig. 1. The plasma is generated in the production region by electron cyclotron resonance (ECR) of a microwave injected along the magnetic field. In the test region where plasma is transported along the field lines from the production region, energetic ions are planned to be produced and measured. The RPA is installed in this position. A traditional ion source with a zeolite emitter [8] will be equipped at the end of the test region. Experimental conditions for plasma production are as follows. The frequency and injection power of the microwave are 2.45 GHz and 1.0 - 6.0 kW. Helium gas is used in the experiment. Operation pressure is 0.19 Pa. We measured electron density and temperature of the bulk plasma by a Langmuir probe for comparison with measurement result of the ion energy analyzer. Under the above conditions, the electron temperature and density in the test region (z = 1.53 m) on the axis of the vacuum vessel (r = 0 m) were about 2 - 8 eV and 5×10^{15} - 5×10^{17} m^{-3}, respectively.

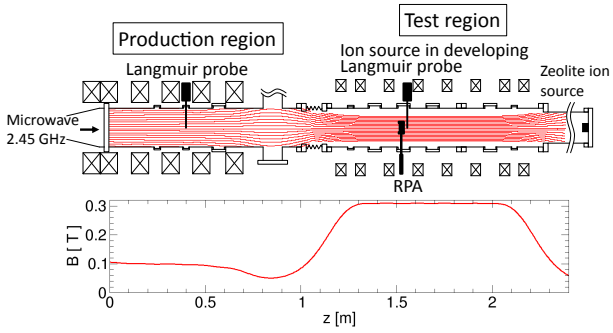

Fig. 1 Schematic diagram of NUMBER and magnetic field strength on the central axis.

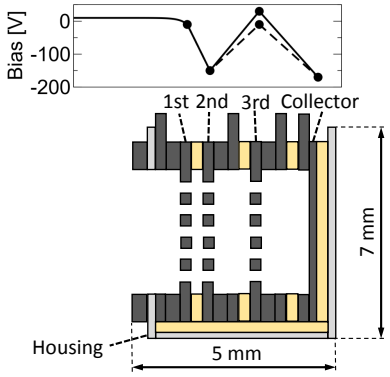

Fig. 2 Schematics of (top) potential of each grid and (bottom) cross-section of retarding potential analyzer (RPA).

3. Method of Measurement

In order to directly measure high energy ions in the plasma, we have developed an ion energy analyzer or an RPA. The analyzer consists of three mesh grids and a collector as shown in Fig. 2. The grid gaps and grid mesh size are determined so that those are sufficiently small compared with the Debye sheath. The first grid (plasma facing grid) is exposed to the highest plasma density, while the density reduces towards the third grid (grid just in front of the collector). Therefore, the grid gap between the first and the second grids is determined using the Debye length for the bulk plasma, the density and temperature of which are 10^{18} m^{-3} and 10 eV. Then the corresponding Debye length is 0.024 mm. Since the grid gap should be smaller than four times the Debye length [9], it was set to 0.075 mm. This gap is maintained by inserting a thin film made of polyimide. Three grids are made of stainless steel, the size of which is 0.04 mm in diameter and 200 meshes per inch. Then the mesh opening 0.087 mm is also satisfies the four times of Debye length condition (< 0.096 mm). Because each mesh is supported by a 0.8 mm thickness washer, the mesh gaps between the second and the third grid and between the third grid and collector are about 1 mm.

In order to minimize the perturbation or shadow effect on the plasma, the analyzer radius is designed to be sufficiently smaller than the plasma radius of about 60 mm. While the clear aperture of the analyzer is 4.5 mm in diameter, outer most diameter including an insulating film and a stainless steel housing is 7 mm. The surface of housing is coated by ceramic cement to electrically isolate the analyzer from the plasma and to protect from the plasma heat flux.

Typical operation of the RPA is as follows. The first grid is kept at the floating potential in order to minimize plasma disturbance due to the electric field inside the analyzer. We apply a negative voltage to the second grid to retard electrons ($V_2 = -150$ V), and sweep the voltage to the third grid to separate ions according to energy (-10 V < V_3 < 30 V). The sweep frequency was 125 Hz to match the sweep frequency of the Langmuir probe.

Ions with energy exceeding potential eV_3 at the 3rd grid can reach the collector, where e is the elementary charge.

4. Results and Discussion

4.1 Current-voltage characteristics

We obtain the ion energy distribution from the depen-

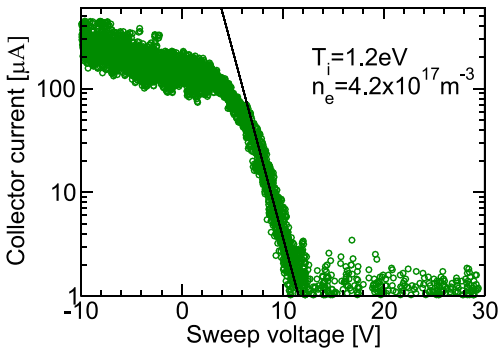

Fig. 3 Example of I-V characteristics.

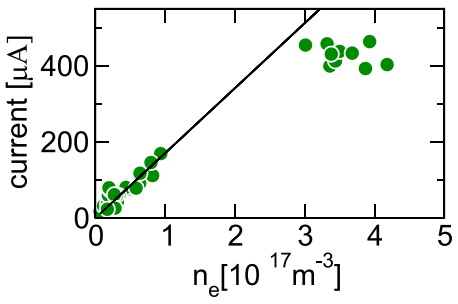

Fig. 4 The collector current at $V_3 = -10$ V as a function of the electron density.

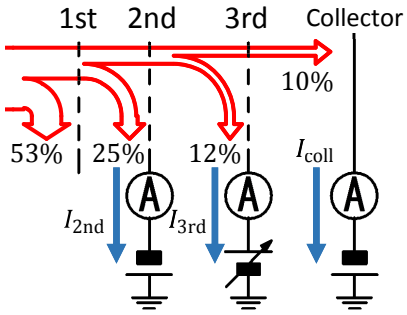

Fig. 5 Ideal fraction of grid and collector currents determined by transparency of each grid.

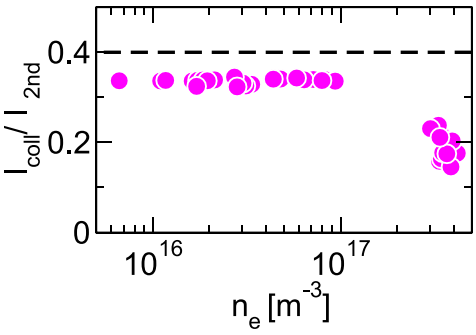

Fig. 6 Ratio of current at $V_3 = -10$ V as a function of the electron density. Dotted line is the ideal value deduced from transparency of grids.

dence of the ion current at the collector on the sweep voltage. Figure 3 shows current-voltage (I-V) characteristics obtained when the electron temperature is 4.0 eV and the electron density is 4.2×10^{17} m^{-3}. We can see that the bulk ion is in Maxwellian with temperature $T_i = 1.2$ eV. Since the plasma is generated by ECR, ion temperature is usually lower than the electron temperature. Therefore, this ion temperature is considered to be an appropriate value. In a range over 15 V in sweep voltage of the third grid, the bulk ion current is under the detection limit. We can conclude the detection limit for energetic ion is about 1 μA from the noise level shown in Fig. 3. Then, a detection limit in current density corresponds to 0.06 A/m^2. This is more than one order smaller than the required value for energetic ion experiment in small devices.

Without applying negative voltage to the collector, we could not obtain appropriate I-V characteristics when the plasma electron density was about 10^{17} m^{-3}. This is because the ions were retarded by the potential generated by the ions accumulated between the 3rd grid and the collector. So, we applied a negative voltage to the collector to accelerate ions from the 3rd grid to the collector and to prevent accumulation of ions. Then, we could obtain appropriate I-V characteristics even for higher density case than 10^{17} m^{-3}.

4.2 Space charge effect

When the I-V characteristics were measured for various bulk densities, saturation of collector current was observed as shown in Fig. 4. For lower density cases $< 1 \times 10^{17}$ m^{-3}, the collector current is proportional to the bulk plasma density as expected. Because ideal collector current for sufficiently negatively biased case is proportional to the ion saturation current of the bulk plasma and is determined by transparency of each grid as shown in Fig. 5, we can expect about 160 μA for 1×10^{17} m^{-3}. The result quantitatively agrees with the expected value. On the other hand, the collector current is saturated around 400 μA for high electron density cases exceeding about 3×10^{17} m^{-3} as shown in Fig. 4. At this time, the electron temperature varied between 3 - 6 eV, and the collector current does not depend on the electron temperature.

In order to identify the cause of this problem, it is necessary to examine the behavior of ions inside the analyzer by experiments and simulations. We improved the measurement circuit so that the current flowing into the grids can be measured as well as the collector current, as shown in Fig. 5.

First, we investigated the electron density and the ratio of the collector current to the second grid current in each measurement condition. As shown in Fig. 6, in the low density region, the ratio is almost constant and is well explained by the geometrical ratio deduced from the transparency of grids shown by the broken line in Fig. 6. On the other hand, the ratio decreased in the high electron density

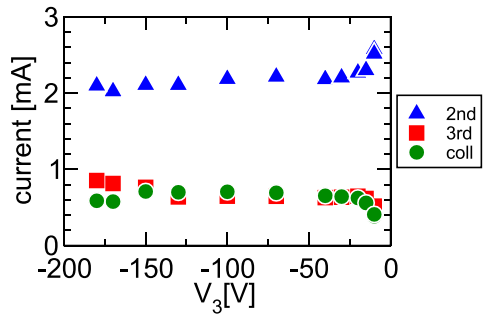

Fig. 7 Grids and collector currents as a function of the third grid voltage.

region, compared to the geometrical ratio. Since the second grid current was almost proportional to the electron density, we can find that ion current decreased between the 2nd grid and the collector in high density cases. We can also find that threshold of electron density at which this phenomenon occurs is between $1 - 3 \times 10^{17}\,\mathrm{m}^{-3}$.

Next, we measured currents of the second and third grids and the collector by changing the third grid biasing voltage while fixing the second grid biasing voltage $V_2 = -150\,\mathrm{V}$. From the measurement by the probe at the same condition, the electron density is $4 \times 10^{17}\,\mathrm{m}^{-3}$ and the electron temperature is 4 eV. When $V_3 > -20\,\mathrm{V}$, the second grid current increased and the 3rd grid and the collector current decreased as shown in Fig. 7. On the other hand, when $V_3 < -20\,\mathrm{V}$, these currents are independent on V_3 and are distributed with the ideal fractions shown in Fig. 5. The sum of currents is almost independent on V_3 even for the case with $V_3 > -20\,\mathrm{V}$. Therefore, when the potential in the third grid is sufficiently higher than that in the second grid, part of the ion current is repelled; not entering into the third grid but reflected back to the second grid.

The behavior of collector current decrease is observed when the bulk plasma density is high enough and the potential difference between the second grid and the third grid is large enough. Therefore, it is thought that ions were retarded by the potential generated by the space charge between the second and third grids. In order to evaluate the behavior of the particles inside the analyzer quantitatively, we carried out a particle-in-cell simulation.

4.3 Simulation by XOOPIC

We examined the behavior of ions inside the analyzer using a particle-in-cell simulation code XOOPIC [10] developed by The Plasma Theory and Simulation Group at Michigan State University. As shown in Fig. 8, the space potential and the ion charge density between the second grid and the collector were calculated. In this simulation region, only ions passing through the 2nd grid were considered. On the other hand, the electrons in the bulk plasma were repelled by the potential of the second grid as confirmed by another calculation with ions and electrons between the bulk plasma and the 2nd grid. In the simulation the time step was 10^{-11} s. Number of calculation cells in the z and r directions were 1000 and 100, respectively. Each grid was modeled with a 0.09 mm diameter hole. The calculation was done for two values of the bulk ion density of the plasma $8 \times 10^{16}\,\mathrm{m}^{-3}$ and $4 \times 10^{17}\,\mathrm{m}^{-3}$, with the same ion temperature of 1 eV. Secondary electron emission on the grid was not included.

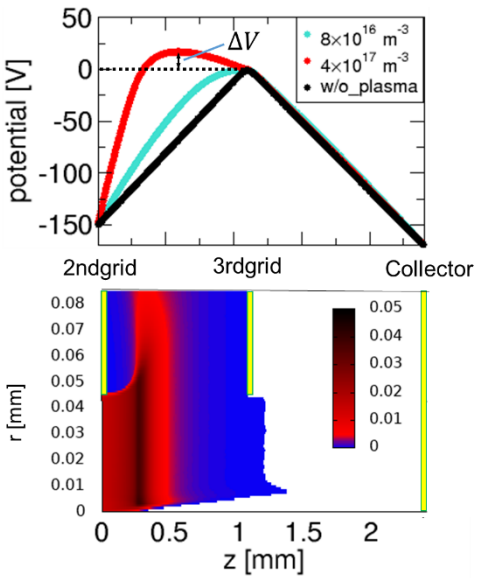

Fig. 8 (Top) potential on the axis and (bottom) ion charge density distribution for ion density of $4 \times 10^{17}\,\mathrm{m}^{-3}$ at 10 μs from start of the calculation. ΔV in the top figure indicates the difference between V_3 and the peak potential.

For the higher ion density case, space charge generated a potential higher than V_3 between the second and the third grids. The generated potential grew with time and became higher than V_3 at 10 ns from start of the calculation. This corresponds to characteristic time scale of 150 eV ions moving between the 2nd grid and the 3rd grid. From this simulation, it was suggested that the ions were retarded by the potential generated by the space charge between the second and third grids. These results are consistent with the threshold density $1 - 3 \times 10^{17}\,\mathrm{m}^{-3}$, obtained from the experimental results shown in Fig. 6. For the purpose of analyzing the bulk ion energy, a scan range $-10\,\mathrm{V} < V_3 < 30\,\mathrm{V}$ was used in the present experiment. Throughout the range, $140\,\mathrm{V} \leq V_3 - V_2 \leq 180\,\mathrm{V}$, the potential increase by the space charge is expected to be almost unchanged, then the ion temperature can be obtained from the I-V characteristics even if the potential is affected by space charge. Detailed discussion will be performed with systematic runs on the simulation, which is our future work. On the other hand, the energetic ion produced by the new method will have energy of several hundred eV or more. The energetic ion density is lower than the bulk ion density, and the potential generated by energetic ions is small. Therefore those ions will overcome the peak poten-

tial generated by space charge; effect of the space charge on the energetic ion detection will be negligible.

5. Conclusions

A retarding potential analyzer (RPA) has been developed for evaluation of the new energetic-ion-production method. From the current-voltage characteristics of RPA obtained at an electron density of about $10^{17}\,\mathrm{m}^{-3}$, the ion temperature 1.2 eV was deduced in a linear device NUMBER for the first time. By measuring the current flowing into each grid, it was found that the current decreased due to the space charge between the 2nd and 3rd grids. The particle-in-cell simulation supported that a potential higher than V_3 was generated due to the space charge inside the analyzer.

While the energetic-ion-production method requires a high density plasma ($\sim 10^{18}\,\mathrm{m}^{-3}$), the experimental results show that the RPA is applicable in terms of both the Debye shielding and perturbation or shadow effect. The detection limit of the RPA ($\sim 0.06\,\mathrm{A/m}^2$) is also determined, which is well below the current required for high energy ion production. Therefore, it is considered that direct detection of energetic ion is promising.

Acknowledgments

This research is partially supported by JSPS KAKENHI Grant Numbers JP19H01869, JP17H06231.

[1] S. Takamura *et al.*, Nucl. Fusion **43**, 393 (2003).
[2] D. Hamada *et al.*, Plasma Fusion Res. **13**, 3401044 (2018).
[3] A. Okamoto *et al.*, Rev. Sci. Instrum. **85**, 02B302 (2014).
[4] R.A. Pitts *et al.*, Rev. Sci. Instrum. **74**, 4644 (2003).
[5] H. Amemiya *et al.*, J. Plasma Fusion Res. **81(7)**, 482 (2005).
[6] T. Baloniak *et al.*, J. Phys. D: Appl. Phys. **43**, 055203 (2010).
[7] D. Brunner *et al.*, Rev. Sci. Instrum. **84**, 033502 (2013).
[8] S. Ohshima *et al.*, Rev. Sci. Instrum. **77**, 03B704 (2006).
[9] I.H. Hutchinson, *Principles of Plasma Diagnostics* (Cambridge University Press, 1987) chapter 3.
[10] J.P. Verboncoeur *et al.*, Comput. Phys. Commun. **87**, 199 (1995).